Determination of GNSS RTK accuracy in various environments

Paul DENYS, Yuxi Jin, Jett Gannaway, Hamish Gibson (New Zealand)

Key words: GNSS, RTK Errors, Multipath, Satellite Visibility, Adverse GNSS Environment,

SUMMARY

Real-Time Kinematic (RTK) is a well-established and versatile Global Navigation Satellite Systems (GNSS) technique widely used in the surveying and geospatial industries. Users are generally aware of GNSS measurement errors caused by satellite geometry, signal transmission, and the local environment, as well as the methods used to mitigate these errors. Most errors are minimized using robust mathematical algorithms, such as double differencing and On-the-Fly techniques, along with appropriate models to account for factors like antenna phase centre and tropospheric delay. However, errors caused by the local environment, such as signal multipath and obstructions from man-made structures or vegetation, remain challenging to address.

This study investigates how reduced signal availability (satellite geometry) in challenging environments affects RTK coordinate accuracy. It quantifies these errors in areas with poor sky visibility and examines the impact of using different satellite constellations, including GPS+Galileo+BDS (GEC), GPS+BDS (GE), and GPS-only (G) configurations.

We established a network of survey marks, including locations with clear sky visibility (0% obstructions) and others affected by tall buildings and vegetation, leading to partial obstructions (20%–50%). The coordinates of these survey marks were determined using a highly redundant network incorporating Total Station measurements, GNSS baseline observations, and Digital Levelling. These network-derived positions were then used to assess positional bias (horizontal and vertical errors) and can be compared to the formal error estimated by the GNSS receiver at the 95% confidence interval.

The results indicate that positioning errors are minimal for survey marks with no obstructions and consistent with manufacturer's accuracy claims. However, as obstructions increase and sky visibility decreases, positional bias grows by a factor of two to three. This demonstrates a clear correlation between reduced sky visibility and an increase in both horizontal and vertical positioning bias.

Measuring GNSS RTK Positioning Errors

Paul DENYS, Yuxi, Jett Gannaway, Hamish Gibson (New Zealand)

1. INTRODUCTION

Modern GNSS technology has significantly expanded the possibilities for positioning and geospatial application, but it also allows users to push the boundaries. Many users have shared experiences of using RTK technology in challenging environments. However, just because the technology can determine a position and display plausible Quality Control (QC) metrics does not guarantee that the computed position is accurate or reliable. While favourable precision statistics often suggest repeatable results, they may still include significant biases caused by signal multipath or reduced satellite availability due to topographical obstructions or vegetation.

For example, positioning errors can occur when an antenna is placed under a protruding veranda, thereby restricting access to GNSS signals and increasing the potential for multipath effects (Figure 1a). Similarly, thick vegetation can interfere with the GNSS signals, reducing positioning accuracy (Figure 1b).

Figure 1: Examples of challenging satellite positioning environments: (a) in the vicinity of buildings including an overhanging veranda (staged), and (b) thick vegetation that interferes with the transmission of the GNSS signal.

Feedback from surveying professionals, including those who hire graduates from the University of Otago's surveying program, highlights another issue: some graduates may place too much trust in GNSS RTK positioning accuracy. They are too accepting of the accuracy and reliability of the technology. This concern is troubling, especially since the Otago surveying program neither teaches nor endorses such practices. However, these issues are likely to be not limited to recent graduates and warrants broader attention.

2. SURVEY DESIGN AND DATA ACQUISITION

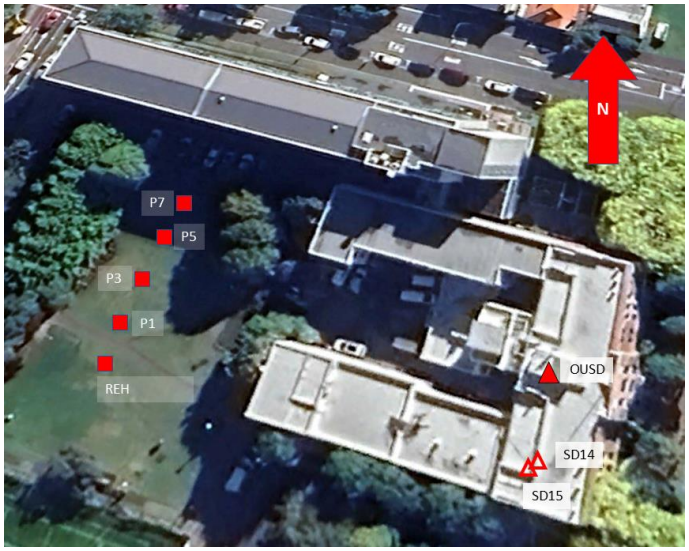

Figure 2: RTK positioning error network. The GNSS base station is on the roof of a three-floor building. The survey marks OUSD, SD14 and SD15 have no sky visibility masking while the survey marks at ground level (REH, P1, P3, P5 and P7) all have some level of sky visibility masking.

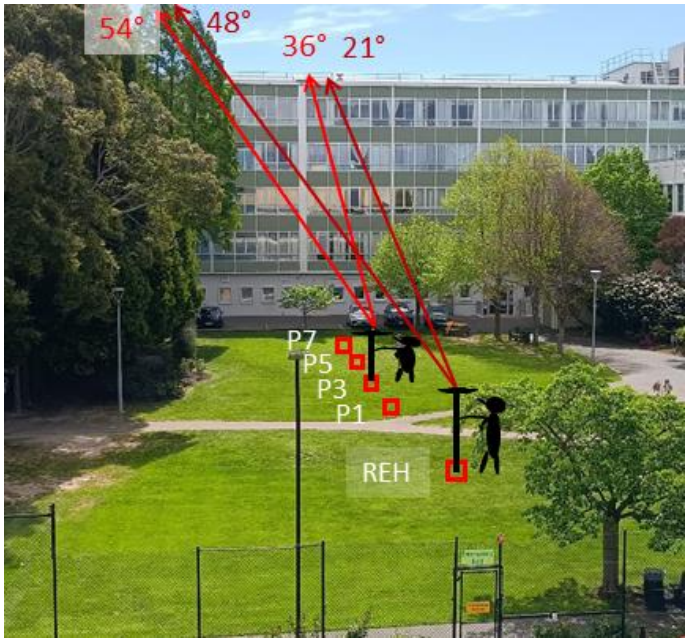

Figure 3: Location of the survey marks showing the increase in sky visibility masking towards the building (background) and the tall trees on the LHS. The building is approximately 18 m high.

A network of survey marks was established within 100 m of a GNSS base station (OUSD) (Figure 2). The base station and two other marks, SD14 and SD15, are located on the roof of a three-story building (approximately 12 m high) and have clear sky visibility with no obstructions above 15°. The positions of all the marks were determined using a combination of total station measurements, GNSS static baseline observations, and height differences measured through digital levelling.

The survey marks on the ground are subject to varying levels of sky visibility obstruction. The amount of obstruction (masking) increased progressively for the marks, REH, P1, P3, P5, and P7 as they approached the building and the tall trees on the left-hand side (Figure 3) This progression is also evident in the sky visibility plots shown in Figure 4.

The roof sites (OUSD, SD14, SD15) had no obstructions (0% masking), while the ground reference site (REH) experienced approximately 19% obstruction, mostly in the northwest quadrant due to the building and trees. The obstructions progressively increased for the other ground marks (P1, P3, P5, and P7) to 24%, 33%, 43%, and 52%, respectively. Initially, the obstructions were primarily to the west, but they

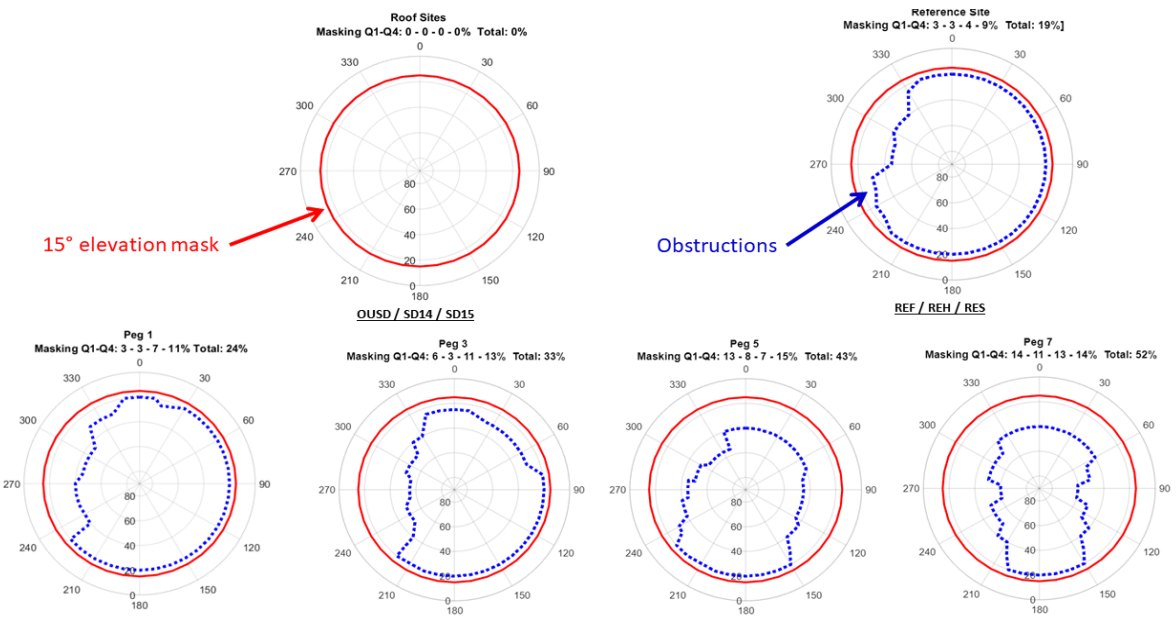

Figure 4: Sky visibility plots. The roof sites (OUSD, SD14, SD15) did not have obstructions above 15° (and the instrument elevation mask was set to 15°). The reference site, REH, had masking above 15° of 19%, while the pegs P1, P3 P5 and P7 had increasing masking of 24%, 23% 43% sand 52% masking.

gradually increased to the north and east. There were no significant obstructions to the south, although satellite signals from this direction were minimal due to the GNSS constellation configuration.

The marks were positioned using a combination of total station measurements, digital leveling, and GNSS static baseline observations. Each mark was occupied multiple times to create a network with a high level of redundancy. Selected GNSS baselines were used to reliably connect the roof sites (OUSD, SD14, SD15) to specific ground sites (Figures 2 and 3). The least squares adjustment of the network resulted in horizontal and vertical coordinate precisions of 1–2 mm at the 95% confidence level.

2.1 Accuracy and precision metrics

Accuracy and precision metrics are widely used to describe the variability of measurements. However, as noted by van Diggelen (1998, 2007), these metrics are often applied inconsistently in both the scientific literature (Deakin and Kildea, 1999) and by GNSS receiver manufacturers. Two common measures of positional accuracy, which account for repeatability and bias, include the root mean square error (rms) and circular error probability (CEP). Using the network coordinates as the true survey mark values, (E_t, N_t, H_t), the circular horizontal and linear vertical root mean square errors, (rms_{Hz}, rms_{Vt}), are given by:

$$rms_{Hz} = \sqrt{\frac{\sum[(E_i - E_t)^2 + (N_i - N_t)^2]}{n}} \quad and \quad rms_{Vt} = \sqrt{\frac{\sum(H_i - H_t)^2}{n}} \qquad (1)$$

where E_i, N_i, H_i are measure coordinates and n is the total number of computed positions. The rms metric calculates the average squared error, while the CEP represents the median horizontal error and is less influenced by large outliers, making it a robust statistic. These metrics can also be expressed at different confidence levels, such as 2drms, R95, R99 (see below), or extended to three dimensions (e.g., spherical error probability, SEP).

For comparison, we also include the receiver-determined position repeatability or precision. This is also known as the formal error and is derived from the RTK position covariance matrix. The circular horizontal standard deviation is a circle with a radius computed from the square root of the sum of the east and north variances, (σ_{Hz}), given by:

$$\sigma_{Hz} = \sqrt{\sigma_E^2 + \sigma_N^2} \qquad (2)$$

Similarly, the linear vertical coordinate standard deviation, (σ_{Vt}), is calculated from the corresponding variance component.

Many of these common metrics have their origins in military positioning and ballistics, as detailed in foundational works by Greenwalt and Shultz (1962), Taub and Thomas (1983), Chin (1987) and Deakin and Kildea (1999). While accurately quantifying positioning accuracy and precision remains essential in surveying applications, the rise of smartphones and personal navigation devices has introduced new accuracy standards. For example, the Japanese mobile phone market uses a 98% confidence interval for its accuracy metrics (van Diggelen, 2007).

Here, we define commonly used accuracy measures:

• Probable Error (PE):	1D	50% (median value)
• Circular Error Probability (CEP)	2D	Circle of radius with 50% probability (median error radius) centred on the true position
• Root Mean Square Error (rms)	1D	Square root of the average of squared errors
• Root Mean Square Error (drms)	2D	Square root of the average of squared horizontal errors
• 2D Root Mean Square Error (2drms)	2D	Twice the rms of the horizontal errors
• R95, R99	2D	Circle of radius with 95% / 99% probability centred on the true position

When calculating these metrics, certain assumptions are made:

1. Positioning measurements follow a normal (Gaussian) distribution.
2. Horizontal positioning errors are approximately circular. Although not strictly accurate, with multi-constellation systems and near-complete satellite availability, position ellipticity is minimal (van Diggelen, 2007). This simplifies the statistical analysis.

Table 1: Common vertical (1D) and horizontal (2D) accuracy measures with their corresponding probabilities and scaling factors to convert from the 1 sigma uncertainty.

Vertical			**Horizontal**		
	Prob (%)	Scale		Prob (%)	Scale
PE	50%	0.6745	1 sigma	39.35%	1.0
1 sigma	68.3%	1.0	CEP	50%	1.177
rms	68.3%	1.0	drms	63.21%	1.414
	95%	1.96	2 sigma	86.47%	2.0
2 sigma	95.45%	2.0	R95	95%	2.448
	99%	2.5758	2drms	98.20%	2.835
3 sigma	99.73%	3.0	3 sigma	98.89%	3.0
			R99	99%	3.035

It is straightforward to compute 1D precision measures (e.g., for easting, northing, or vertical components). However, calculating metrics for 2D (horizontal) or 3D positioning is more complex. For vertical errors (1D), probabilities can be converted using the normal distribution's scaling factors (Table 1). For horizontal positioning (2D), the chi-squared (χ^2) distribution is used to combine two normally distributed variables (easting and northing), as expressed by van Diggelen (2007):

$$p = \chi^2(R^2, 2) \qquad (3)$$

Here, p is the probability level, and R is the radius or scaling factor. For example:

$$R95 = R\sigma_x = 2.448\sigma_x \qquad (4)$$

Conversions between metrics, such as from CEP to 2drms, are also possible:

$$2drms = \frac{2.835}{1.177} CEP = 2.409 CEP \qquad (5)$$

In this study, we use 2drms, CEP, and 95% confidence interval (CI), determined by the receiver, to compare horizontal accuracy.

3. POSITIONAL PERFORMANCE OF TEST ENVIRONMENTS

Data was collected from the test sites using different satellite constellations: GPS only (G) and a combination of GPGS and Galileo (GE) and GPS, Galileo, and BDS (GEC). The test sites included two distinct environments:

1. **Roof Sites:** These sites had no significant obstructions and zero masking.
2. **Ground Sites:** These sites experienced increasing levels of environmental obstructions, ranging from 19% to 52% masking.

The roof sites served as reference points where we expected optimal positioning performance, with the highest accuracy and reliability. In contrast, the ground sites were subject to environmental masking, which was anticipated to affect performance due to three main factors:

1. A reduction in the number of observable satellites.
2. An increase in multipath errors.
3. Higher measurement noise caused by vegetation interference e.g. leaves.

These three sources of bias were expected to combine and result in decreased overall positioning accuracy and reliability. However, this study did not attempt to separate these biases individually.

3.1 Roof Sites – Zero satellite visibility masking

Two types of GNSS receivers, the Trimble R6 and R10, were tested on the roof sites using the following satellite constellations: GPS only (G), GPS + Galileo (GE), and GPS + Galileo + BDS (GEC). Positioning data was collected at one-minute intervals over several days. The median number of satellites observed increased from 8 for the Trimble R6 with GPS only (G) to 21 for the Trimble R10 tracking three constellations (GEC) (Table 2).

No statistically significant differences were found between the GPS-only positioning results from either of the R6 and R10 receivers. However, adding one or two constellations improved both vertical and horizontal positioning accuracy. The vertical accuracy improved by approximately 25%, from 12–13 mm to 9 mm (95% CI), while the horizontal accuracy improved from 8 mm to 5–6 mm (95% CI) (Table 2).

The receivers also calculate formal vertical and horizontal positioning errors, represented as a grey line in Figures 5 and 6. Outlier positions, marked with red "+" symbols, are those where the position error exceeded the receiver's formal 95% confidence interval. In practical fieldwork, this precision metric is often used to assess the reliability of computed positions, making it important to evaluate its validity.

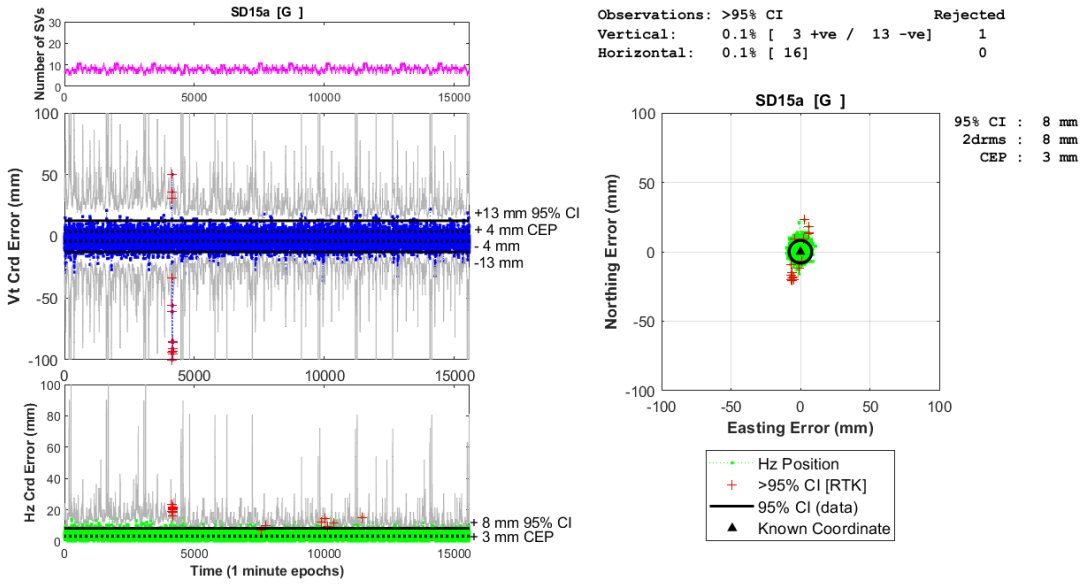

Figure 5: Height [blue dots] and horizontal [green dots] positions for the GPS only constellation, Trimble R10 [G]. The grey line represents the R10 computed 95% CI (formal) error. The red "+" are outlier positions that lie outside the 95% CI for which there are 0.1% (both vertical and horizontal, totals 16). There was 1 rejected position being greater than 100 mm error.

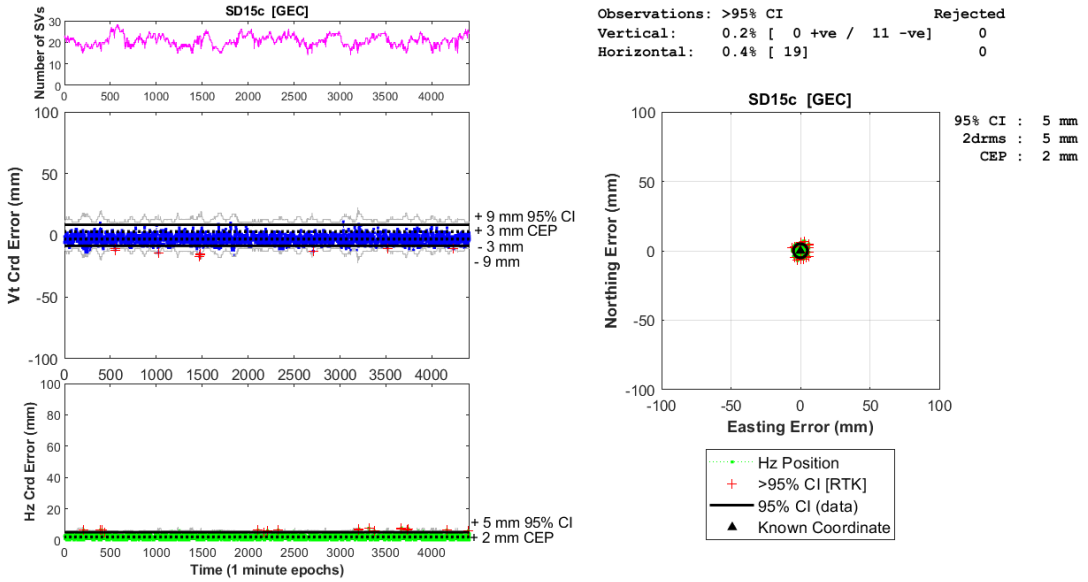

Figure 6: Height [blue dots] and horizontal [green dots] positions for the GPS + Galileo + BDS constellations, Trimble R10 [GEC]. The grey line represents the R10 computed 95% CI (formal) error. The red "+" are outlier positions that lie outside the 95% CI for which there are 0.2% (vertical, total 11) and 0.4% (Horizontal, total 19). There were no rejected observations (>100 mm error).

A small percentage of the observations exceeded the formal 95% confidence interval, although most vertical errors were negative (Table 2). Figures 5 and 6 show the time series for vertical positions and horizontal plots for the R10 with GPS only (G) and with all constellations (GEC), respectively.

Table 2: Summary data for the roof sites including the median number of satellites tracked, total number of observations, the vertical and horizontal accuracy as determined by the 95% CI and CEP metrics and the number of outlier observations greater than the receiver's formal error (95% CI).

	R6 [G]	R10 [G]	R10 [GE]	R10 [GEC]
SVs (median)	8	8	14	21
n	5801	15584	4323	4409
Vertical				
95% CI (mm)	12	13	9	9
CEP (mm)	4	4	3	3
Obs > 95% CI +ve	7	3	0	0
-ve	5	13	10	11
Horizontal				
95% CI (mm)	8	8	6	5
CEP (mm)	3	3	2	2
Obs > 95% CI	12	16	20	19

A noteworthy observation is the significant improvement in formal error (95% CI) between the R10 (G) (Figure 5) and the R10 (GEC) (Figure 6). Including additional constellations, which increased the median number of satellites from 8 to 21, clearly enhanced the formal error computed by the receiver. Similar improvements were observed when one additional constellation was added (GE), increasing the median number of satellites to 14.

3.2 Ground Sites: 19% – 52% satellite visibility masking

The ground sites included a reference mark (REH), where a receiver was continuously operating, along with several test marks that experienced progressively less sky visibility. Figures 7 and 8 show data from two of these sites, REH and P3. Compared to the roof sites, the ground sites tracked about half as many satellites. As expected, the median number of satellites decreased as the obstructions increased (Table 3).

At the reference site (REH), where obstructions were around 19%, the vertical and horizontal accuracies were reduced by factors of two and three, resulting in accuracies of 21 mm and 19 mm, respectively (95% CI). For the other ground sites, as obstructions increased from 19% to 52%, vertical and horizontal precisions progressively worsened, reaching unacceptably high errors of approximately 100 mm (95% CI) at the most obstructed site (P7, with 52% obstructions) (Table 3).

The positioning results (not tabulated) using only the GPS constellation were even poorer. While these results align with expectations, the key finding is that even with multi-constellation solutions, positioning accuracy is significantly impacted by relatively small increases in obstructions. For example, a 20% obstruction level reduces accuracy by a factor of two to three.

Table 3: Summary data for the ground sites including the median number of satellites tracked, obstructions (%), the vertical and horizontal accuracy as determined by the 95% CI and CEP metrics, the number of outlier observations greater than the receivers' formal error (95% CI).

	REH [GEC]	P1 [GEC]	P3 [GEC]	P5 [GEC]	P7 [GEC]
SVs (median)	16	13	12	12	9
Obstruction (%)	19	24	33	43	52
Vertical					
95% CI (mm)	21	49	57	82	112
CEP (mm)	5	10	16	28	52
Obs > 95% CI +ve	1099	51	450	289	116
-ve	737	0	6	13	2
Horizontal					
95% CI (mm)	19	36	44	65	71
CEP	4	13	13	24	26
Obs > 95% CI	2748	240	1094	787	150

As expected, there is an increase in outlier positions with decreasing accuracy. Additionally, the number of rejected positions (with errors greater than 100 mm) also increases. Table 3 shows the number of outliers exceeding the 95% confidence interval (CI). For the roof sites (Section 2.1), the vertical component showed a slight bias towards negative errors. However, at the ground sites, as obstructions increased, the majority of the vertical errors are positive. While there seems to be a decrease in outlier observations at sites P3, P5, and P7, this is actually due to more instances where the receiver could not calculate a position because of increased obstructions. As a result, the total number of positions recorded were fewer, and the errors became larger.

A key difference between the ground sites REH (Figure 7) and P3 (Figure 8) is the increase in outlier positions, based on the receiver's computed (formal) error (95% CI). Clearly, the formal error underestimates the position precision, with outlier observations at REH being 30% for the vertical component and 46% for the horizontal component. In Figure 7 (REH), the outlier observations are spread across the entire error distribution, with both small and large errors. There is also a noticeable north-south bias in the horizontal errors, and a positive bias in the vertical errors (1099 positive vs. 797 negative). This suggests that the RTK positioning model is not accounting for either the reduced number of available satellites (geometry) or the increased measurement noise from multipath and/or vegetation interference.

In contrast, the results at P3 show an improvement (decrease) in the number of outliers, with vertical and horizontal outlier observations at 15% and 35%, respectively. However, the receiver's computed 95% CI formal uncertainty are larger compared to REH, which leads to fewer outliers being identified. Unlike REH, the positioning model at P3 appears more realistic,

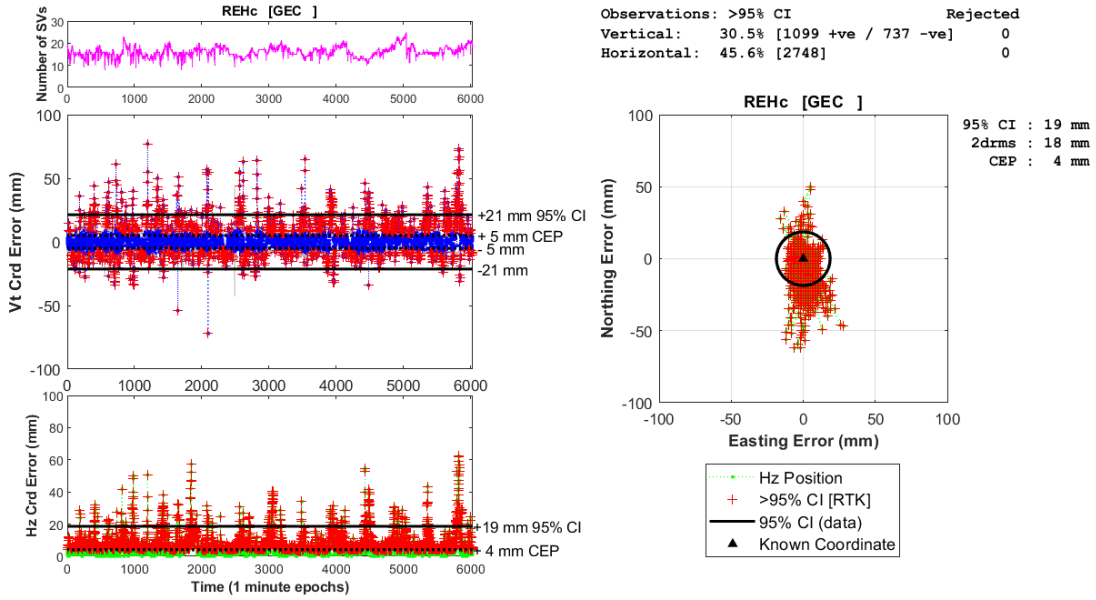

Figure 7: Height [blue dots] and horizontal [green dots] positions for the GPS + Galileo + BDS constellations, Trimble R10 [GEC]. The grey line represents the R10 computed 95% CI (formal) error. The red "+" are outlier positions that lie outside the 95% CI for which there are 30% (vertical, total 1736) and 46% (horizontal, total 2748).

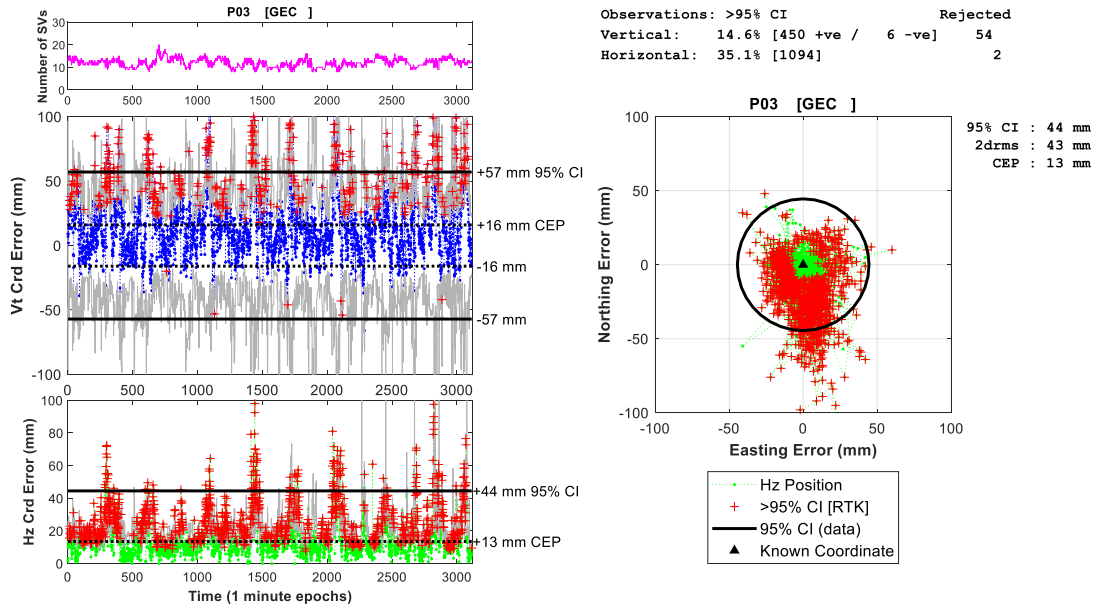

Figure 8: Height [blue dots] and horizontal [green dots] positions for the GPS + Galileo + BDS constellations, Trimble R10 [GEC]. The grey line represents the R10 computed 95% CI (formal) error. The red "+" are outlier positions that lie outside the 95% CI for which there are 15% (vertical, total 450) and 35% (horizontal, total 1094). There was 54 / 2 rejected vertical / horizontal positions being greater than 100 mm error.

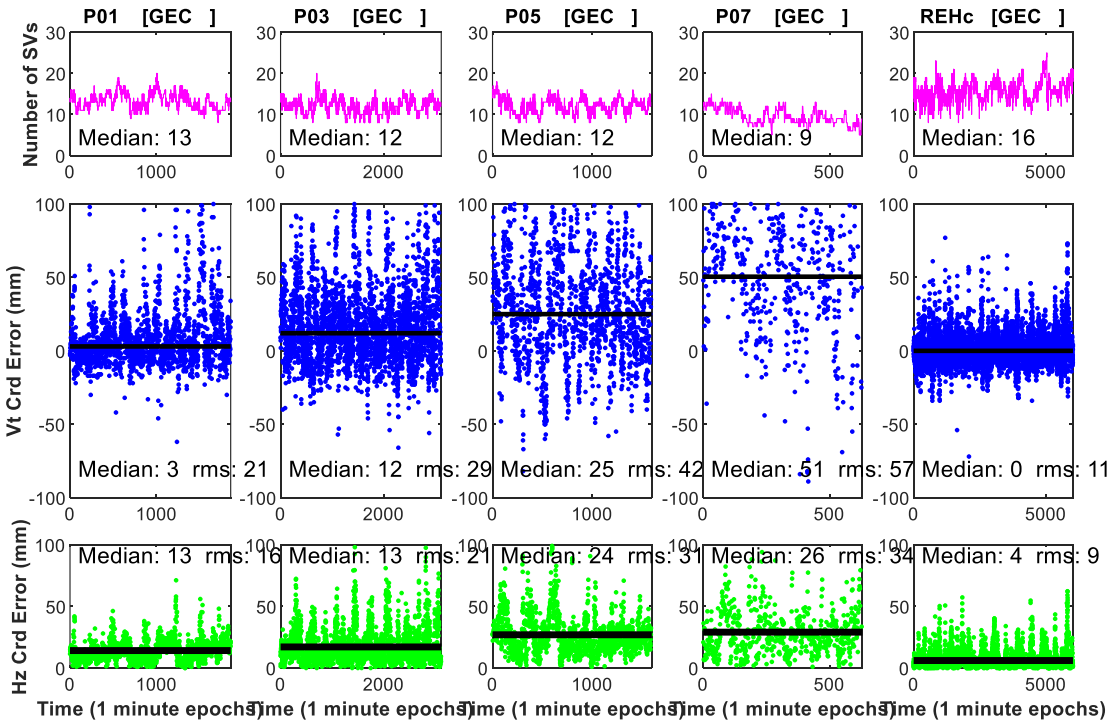

Figure 9: Summary plots for the sites P1, P3, P5, P7 and REH. Shown are the median number of satellites (top row), median coordinate error and rms for the vertical (middle row) and horizontal (bottom row) coordinate error.

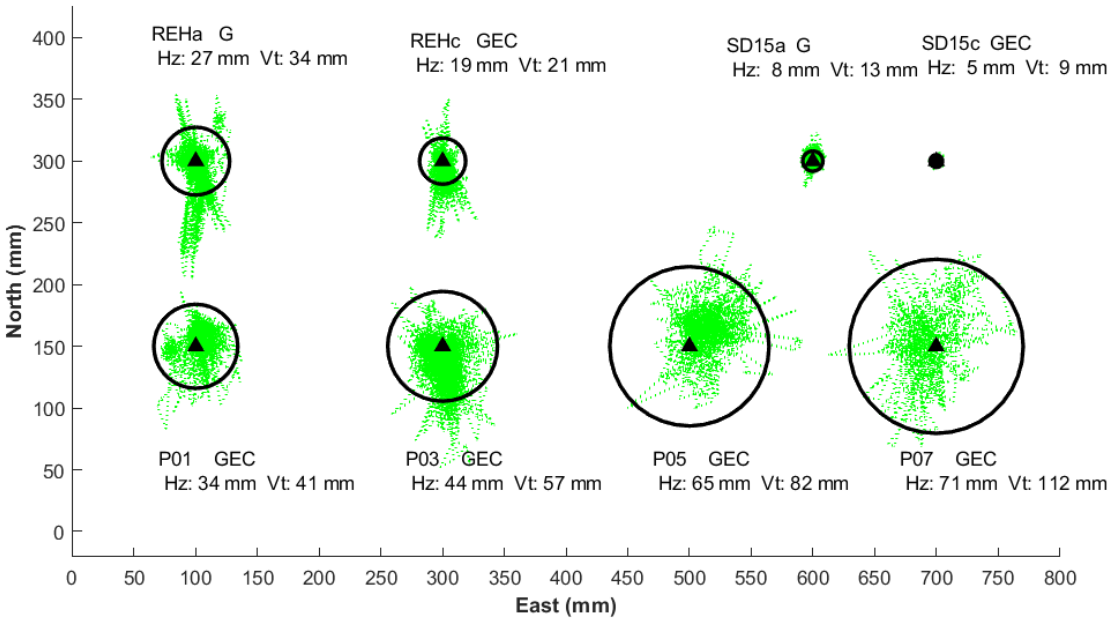

Figure 10: Plots of horizontal position for the sites reference site REH (G and GEC constellations); the roof sites SD15 (G and GEC constellations); and the ground sites P1, P3, P5, P7 (GEC constellations only). The black circle represents the 95% CI horizontal coordinate uncertainty, and the 95% CI numerical uncertainties are given for both the horizontal and vertical coordinate components.

and if we assume that the measurement noise (due to multipath and vegetation) is similar at both sites, the main factor causing the difference is the number of available satellites. The median number of satellites tracked decreased from 16 at REH to 12 at P3.

To compare the performance across all five ground sites (P1, P3, P5, P7, and REH), Figure 9 provides a summary. The figure shows the number of satellites tracked (top row), vertical coordinate errors (middle row), and horizontal coordinate errors (bottom row) for each site. The median bias and root mean square (rms) values for vertical and horizontal errors are also shown. The degradation in positioning accuracy is clearly shown for the sites P1 – P7 compared to the reference site REH.

Finally, Figure 10 shows horizontal plots for the roof site (SD15), reference site (REH), and the ground sites (P1 – P7). The plots for both the GPS-only (G) and GPS + Galileo + BDS (GEC) constellations are shown for SD15 and REH, while only the GEC constellation is shown for the other sites. The black circle represents the 95% CI uncertainty in the horizontal component, and both horizontal and vertical uncertainty values (95% CI) are also included for each site.

The roof site (SD15) performed as expected, with virtually no obstructions, minimal multipath and no vegetation interference, resulting in 95% CI horizontal uncertainties of around 10 mm. There were a small number of outlier positions. When sky masking increased to around 20%, the 95% CI uncertainty doubled to around 20 mm for the GEC constellation and 20-30 mm for the GPS-only constellation. For the remaining ground sites, where sky visibility ranged from 24% (P3) to 52% (P7), the 95% CI uncertainty increased from 30-40 mm to around 100 mm. `

4. CONCLUSIONS

GNSS RTK positioning accuracy is generally assumed to align with the specifications provided by GNSS manufacturers. For locations with no obstructions and clear sky visibility, these accuracy levels are easily achieved. In such conditions, the reported RTK accuracies are consistent, and a slight improvement is observed when using multi-constellation solutions (e.g., GPS combined with Galileo (GE) or GPS, Galileo, and BeiDou (GEC)) compared to GPS-only solutions.

However, even minor obstructions (e.g., 20% blockage) lead to a significant reduction in accuracy, with errors increasing by a factor of 2–3. This degradation is primarily attributed to three factors: poorer satellite geometry due to fewer tracked satellites, increased signal noise caused by multipath effects, and signal interference and or degradation from vegetation. While horizontal positioning errors occur in all directions, there is a slight bias predominantly in the north-south direction. For the vertical component, the errors tend to show a positive bias.

The results of this experiment are specific to this (challenging) environment, which is influenced by the presence of both tall buildings and vegetation. Since positioning accuracy is partly dependent on geometry, a different environmental layout—such as vegetation aligned in

an east-west direction—would likely produce a different error pattern. Similarly, obstructions in the surrounding environment, including buildings and/or vegetation, alter multipath errors and GNSS signal interference, leading to a different positioning bias. While the specific characteristics of the environment influence this bias, a key observation is that both horizontal and vertical positioning biases tend to increase as the environment becomes more challenging. As sky obstructions or sky masking increases, the magnitude of positional errors is also expected to increase.

As the level of satellite obstruction increases (e.g., from 19% to 52%), both vertical and horizontal errors rise rapidly—from approximately 20–30 mm at 19% obstruction to around 100 mm at 52% obstruction. Additionally, higher levels of obstruction reduce the receivers' ability to reliably resolve positions.

REFERENCES

Chin, G. Y., (1987). *Two-dimensional measures of accuracy in navigational systems,* (No. DOT-TSC-RSPA-87-1). United States. Dept. of Transportation. Office of Research and Special Programs. URL: rosap.ntl.bts.gov/view/dot/9683/dot_9683_DS1.pdf. Accessed November 2024.

Deakin, R. E. and Kildea, D. G., (1999). A note on standard deviation and RMS. *Australian Surveyor*, *44*(1), 74-79.

Greenwalt, C. R., and Shultz, M. E. (1962). *Principles of error theory and cartographic applications*, Tech Report No. 96, United States Air Force, Aeronautical Chart and Information Center. *Louis, MO, USA*. URL: apps.dtic.mil/sti/tr/pdf/AD0276978.pdf. Accessed November 2024

Taub, A. E. and Thomas, M. A. (1983). *Confidence Intervals for CEP when the errors are elliptical normal*. Tech. Rep. No. NSWC/TR-83-205. Dahlgren, VA: US Naval Surface Weapons Center, Dahlgren Division. URL: apps.dtic.mil/sti/tr/pdf/ADA153828.pdf. Accessed November 2024.

van Diggelen, F., (1998). GNSS Accuracy, Lies, Damn Lies and Statistics, *GPS World*, *9*(1), 41-45. URL: www.gpsworld.com/gps-accuracy-lies-damn-lies-and-statistics/, Accessed November 2024

van Diggelen, F., (2007). GNSS Accuracy, Lies, Damn Lies and Statistics, *GPS World*, *18*(1), 26-33. URL: www.gpsworld.com/gpsgnss-accuracy-lies-damn-lies-and-statistics-1134/, Accessed November 2024.

BIOGRAPHICAL NOTES

Paul Denys: I have been an academic staff member at the School of Surveying, Otago University since 1995, teaching papers in Survey Methods and Survey Mathematics. My primary interest is GNSS positioning and geodetic data analysis with a focus on RTK positioning errors and active deformation. New Zealand offers an excellent opportunity to study and understand the broad scale deformation of the Australian-Pacific plate boundary as well as focusing on specific problems: Central Otago and Cascade deformation, Southern Alps uplift and sea level rise. I have also been involved with the geodetic analysis of recent major earthquake events in New Zealand and including the maintenance of the geodetic infrastructure.

CONTACTS

Dr. Paul H. Denys
School of Surveying
University of Otago
PO Box 56
Dunedin
NEW ZEALAND
Tel.: +64 3 479 7596
Email: pdenys@surveying.otago.ac.nz
Web site: www.otago.ac.nz/surveying